



Novel *GATA6-FOXO1* fusions in a subset of epithelioid hemangioma

Cristina R. Antonescu¹ · Shih-Chiang Huang² · Yun-Shao Sung¹ · Lei Zhang¹ · Burkhard M. Helmke³ · Martina Kirchner⁴ · Albrecht Stenzinger⁴ · Gunhild Mechttersheimer⁴

Received: 24 August 2020 / Revised: 7 November 2020 / Accepted: 10 November 2020 / Published online: 14 December 2020
© The Author(s), under exclusive licence to United States & Canadian Academy of Pathology 2020

Abstract

The genetic hallmark of epithelioid hemangioma (EH) is the presence of recurrent gene fusions involving *FOS* and *FOSB* transcription factors, which occur in one-third of the cases. Certain clinical, pathologic, and genotypic correlations have been described, with *FOS*-related fusions being more often detected in skeletal and cellular variants of EH, while *FOSB* gene rearrangements are more commonly associated with atypical histologic features and penile location. These fusions are infrequently detected in the cutaneous or head and neck EH. Overall, two-thirds of EH lack these canonical fusions and remain difficult to classify, especially when associated with atypical features and/or clinical presentations. Triggered by an index case of an intravascular soft tissue EH with a novel *GATA6-FOXO1* gene fusion by targeted RNA sequencing (Archer® FusionPlex® Sarcoma Panel), we have investigated 27 additional EH cases negative for *FOS* and *FOSB* gene rearrangements for this novel abnormality to determine its recurrent potential, and its association with clinical and pathologic features. Four additional EH cases were found to display *GATA6-FOXO1* fusions (18%). There were three females and two males, with a mean age of 32 years old. Three lesions occurred in the head and neck (dura, nasopharyngeal, and cheek), one in the back and one in the leg. Two of these lesions were cutaneous and one was intravascular in the subcutis of the leg. Microscopically, the tumors showed a variegated morphology, with alternating vasoformative and solid components, extravasated red blood cells and mild to moderate cytologic atypia. None showed brisk mitotic activity or necrosis. Tumors were negative for *FOS* and *FOSB* by immunohistochemistry. In conclusion, we report a new *GATA6-FOXO1* fusion in a subset of EH, with a predilection for skin, and head and neck location. The relationship of this novel molecular subset with the more common *FOS/FOSB* fusion-positive EH remains to be determined.

Introduction

Epithelioid hemangioma (EH) is an uncommon but distinctive vascular neoplasm, displaying well-formed vascular

channels lined by prominent epithelioid endothelial cells [1]. The diagnosis of EH remains challenging due to its wide histologic spectrum, including a cellular/solid growth, a heavy inflammatory infiltrate, and occasional intravascular growth. The diverse histologic appearances are also reflected by the variety of its previous designations, such as intravenous atypical vascular proliferation [2], angiolymphoid hyperplasia with eosinophilia (ALHE) [3–5], inflammatory angiomatous nodule [6], and histiocytoid hemangioma [7]. Moreover, a subset of cases, particularly the ones arising in the bone, display an aggressive clinical and radiographic presentation, being associated with a high local recurrence rate and regional multifocality, which may suggest malignancy; however, they lack distant metastatic potential or tumor-related deaths [8]. Although the pathogenesis of EH has been long controversial, with some early reports suggesting that in particular skeletal EH represents a variant of epithelioid hemangioendothelioma (EHE), thus having metastatic potential [9], it is now widely recognized that EH is a benign, locally aggressive neoplasm [1, 10].

Supplementary information The online version of this article (<https://doi.org/10.1038/s41379-020-00723-4>) contains supplementary material, which is available to authorized users.

✉ Cristina R. Antonescu
antonesc@mskcc.org

- ¹ Department of Pathology, Memorial Sloan Kettering Cancer Center, New York, NY, USA
- ² Department of Pathology, Chang Gung Memorial Hospital, Chang Gung University, College of Medicine, Taoyuan, Taiwan
- ³ Institute of Pathology, Elbe Clinic, Stade-Buxtehude, Stade, Germany
- ⁴ Institute of Pathology, University Hospital Heidelberg, Heidelberg, Germany

The discovery of recurrent *FOS* and *FOSB* gene fusions has strengthened its stand-alone pathogenesis, distinct from other look-alike malignant epithelioid vascular lesions, such as EHE or angiosarcoma (AS). However, only one-third of EH display *FOS/FOSB* gene alterations [11, 12], although the incidence varies significantly with anatomic locations, with skeletal EH having the highest proportion of fusion positive (>70%) [13]. The pathogenesis of *FOS/FOSB* fusion-negative EH cases remains undetermined, especially in cases that occur at nonskeletal locations. In this study, we investigate a large cohort of EH cases lacking these canonical alterations, for the presence of a novel *GATA6-FOXO1* fusion.

Material and methods

Patient selection and pathologic review

The study was initiated by an index case of an EH lacking the canonical *FOS* and *FOSB* gene rearrangements, but instead harboring a novel gene fusion. The case occurred in a 42-year-old female presenting with a painful lesion in her right leg. The tumor was located superficially in the subcutis and measured 1 cm in greatest dimension (case 1, Table 1). Prompted by this result, we have then searched the MSKCC Pathology Department and the personal consultation files of

the corresponding author (CRA) for the diagnosis of EH during a 15-year period (2005–2020), which had molecular results or material available for genetic work-up. A total of 28 EH were selected that were negative for gene alterations in *FOS* and *FOSB* genes by fluorescence in situ hybridization (FISH) or targeted RNA-sequencing methods. The study was approved by the Institutional Review Board.

Hematoxylin and eosin (H&E)-stained slides and immunohistochemical stains were rereviewed. The tumors were assessed for growth pattern, degree of vasof ormation, presence of blister cells (or intracytoplasmic vacuoles), cytomorphology, cellularity, nuclear features, including nuclear contour, chromatin pattern, pleomorphism, and presence of nucleoli, mitotic activity, and necrosis. In addition, the lesions were examined for the presence and type of inflammatory infiltrate and extracellular stroma. The endothelial differentiation was confirmed by CD31, CD34, and ERG immunohistochemistry.

Fluorescence in situ hybridization

Subsequent to the results obtained from targeted RNA sequencing in the index case, all tumors were tested by FISH for *FOXO1* and *GATA6* gene abnormalities. Custom probes made by bacterial artificial chromosomes (BAC) clones flanking the *FOXO1* and *GATA6* genes of interest, according to UCSC genome browser (<http://genome.ucsc.edu>) and

Table 1 Clinicopathologic features of EH characterized by *GATA6-FOXO1* fusions.

EH#	Age/sex	Site/size/procedure/FU	Microscopic features	IHC positive
1	42/F	R leg, subcutis 1 cm Resection, negative margins	Biphasic, vasof ormation and solid growth Intravascular Abundant inflammation (lympho-plasma cells), extravasated red blood cells 1 MF/10 HPFs, mild atypia	CD31, CD34, ERG
2	32/M	Cheek, skin 1.2 cm Resection, negative margin NED 6 months	Biphasic, vasof ormation and solid growth Scant to no inflammation Limited extravasation 2 MF/10 HPFs, mild atypia	CD31, ERG
3	33/F	Dura 3 × 2.5 × 1 cm aggregate Craniotomy, intrasiesional resection NED 36 months	Biphasic, vasof ormation and solid growth Epithelioid, ovoid to spindling (short fascicles) Abundant extravasated blood Scant acute inflammation 2 MF/10 HPFs, moderate atypia	CD31, CD34
4	42/F	H&N, nasopharyngeal 2.4 cm Biopsy only AWD 48 months	Scant vasof ormation Epithelioid, solid, nodular Scant to no inflammation Moderate extravasated blood, 1 MF/10 HPFs, mild atypia	CD31, ERG
5	15/M	Left upper back, skin 0.5 × 0.3 cm Incomplete resection	Biphasic, vasof ormation and solid growth Moderate extravasated blood Scattered eosinophils 2 MF/10 HPFs, moderate nuclear atypia	CD31, ERG

FU follow-up, NED no evidence of disease, AWD alive with disease.

obtained from BACPAC sources of Children's Hospital of Oakland Research Institute (Oakland, CA; <https://bacpa.cresources.org/>; Supplementary Table 1). DNA from each BAC was isolated according to the manufacturer's instructions. The BAC clones were labeled with fluorochromes (fluorescent-labeled dUTPs, Enzo Life Sciences, New York, NY) by nick translation, and validated on normal metaphase chromosomes. The 4- μ m-thick FFPE slides were deparaffinized, pretreated, and hybridized with denatured probes. After overnight incubation, the slides were washed, stained with 4',6-diamidino-2-phenylindole, mounted with an anti-fade solution, and then examined on a Zeiss fluorescence microscope (Zeiss Axioplan, Oberkochen, Germany) controlled by Isis 5 software (Metasystems). Two hundred successive nuclei were examined using a Zeiss fluorescence microscope (Zeiss Axioplan, Oberkochen, Germany), controlled by Isis 5 software (Metasystems, Newton, MA). Cases were first tested for *FOXO1* break-apart signals. If positive, a follow-up three-color FISH fusion assay was performed, using two-color for *GATA6* (red, centromeric; green, telomeric), and one-color for *FOXO1* (orange centromeric). To avoid false-negative results due to an abundant inflammatory component intermixed in some cases, a total of 300 cells were counted in screening areas that were carefully circled on H&E as enriched in lesional cells. A positive score was interpreted when at least 20% of the nuclei showed either a break apart or a come-together signal. Nuclei with incomplete set of signals were omitted from the score.

Targeted RNA sequencing

Only one case had adequate material to be studied by RNA sequencing. The index case was tested by anchored multiplex polymerase chain reaction-based NGS using standard protocols according to the manufacturer. RNA extraction from archival material, library preparation, and semiconductor sequencing were performed, as described previously [14, 15]. In short, tumor tissue was macrodissected to achieve a histological tumor cell content of at least 15%. The extraction was carried out with the automated Maxwell® 16 Research extraction system (Promega, Madison, WI, USA) and the Maxwell® 16 FFPE Plus LEV RNA Purification Kit following the manufacturer's instructions. The sample was then digested with the TURBO DNA-free™ Kit (Thermo Fisher Scientific, Waltham, MA, USA) to obtain DNA-free RNA. The concentration of RNA was measured fluorimetrically (QuBit 2.0 RNA high sensitivity kit, Thermo Fisher Scientific).

For enriched cDNA library preparation, the multiplex PCR-based Ion Torrent AmpliSeq™ technology (Life Technologies, Thermo Fisher Scientific) with the Archer® FusionPlex® Sarcoma kit (Archer® DX, Boulder, CO, USA)

was used according to the manufacturer's instructions, and as described previously [16].

The data were analyzed with the Archer® analysis software (Version 5.1; Archer® DX) for the presence of gene fusions. The sequence quality for each sample was assessed by the following criteria: >10% or at least 150,000 unique fragments, >50 average unique RNA start sites per gene-specific primer 2 (GSP2) control and on-target deduplication ratio <40 [16].

Results

We have identified 28 cases of EH from our files that were negative for *FOS* and *FOSB* gene rearrangements, and had tissue for additional molecular work-up. Of these, five (18%) cases showed the presence of a *GATA6-FOXO1* fusion. In addition, six ALHE cases, mostly from the head and neck location, were also tested.

Clinical and histologic features of *GATA6-FOXO1* fusion-positive EHs

There were three females and two males, with an age range at diagnosis of 15–42 years (mean, 32; median, 33). Three lesions occurred in the head and neck, including: dura, nasopharyngeal, and cheek. One case each occurred in the back and in the leg. Two of these lesions were cutaneous and one was intravascular (index case #1, involving subcutis of the leg). The tumor size ranged from 0.5–3.0 cm (mean 1.2 cm; Table 1). All except one of the lesions were surgically resected, two of them with negative margins, and two were incompletely or intralesionally excised. Follow-up was available in two of these patients, being with no evidence of disease at 6 and 36 months follow-up (Table 1). One tumor (case #4, a nasopharyngeal lesion) was only biopsied and the patient has been followed with periodical imaging, with only minimal increase in size from 2.4 to 3.0 cm over the 4-year follow-up.

Microscopically, the tumors showed a variegated morphology, with alternating vasoformative areas and solid components. In fact, all except one case showed biphasic architectural patterns, with large solid sheets of epithelioid cells adjacent to areas that were predominantly vasoformative (Figs. 1 and 2, and Table 1). The vasoformation was represented by well-formed vascular channels with irregular lumina or inter-anastomosing sinusoidal vessels (Figs. 1 and 2). One tumor showed very scant evidence of vascular channel formation. Most cases showed ample evidence of extravasated red blood cells (Figs. 1 and 2). Other typical microscopic features of EH, such as the so-called “tombstone pattern” of hobnailed endothelial cells protruding into the vascular lumina were not observed.

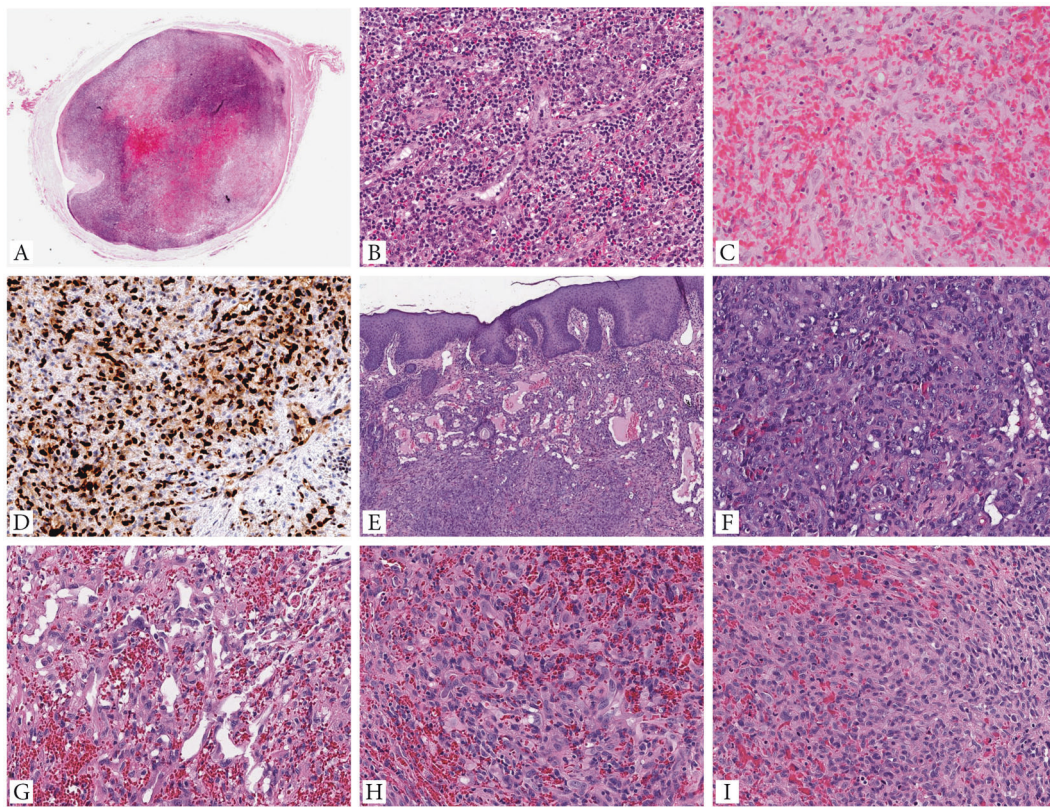


Fig. 1 Morphologic spectrum of EH cases with *GATA6-FOXO1* fusions. **A–D** Intravascular EH presenting as a 1 cm painful nodule in the subcutis of the right leg of a 42-year-old female (case 1, index case). **A** Whole mount showing an intravascular lesion with variegated cellularity and central hemorrhage. **B** High power of the increased cellularity component showing well-formed branching vascular channels, surrounded by brisk lympho-plasmacytic infiltrate. **C** Central hemorrhagic area is composed of epithelioid endothelial cells arranged in cords, sheets, or ill-defined lumina, obscured by abundant extravasated erythrocytes. **D** Tumor cells are strongly and diffusely positive

for ERG. **E, F** (Case 2, cheek) cutaneous EH showing a biphasic architectural pattern, with well-defined vascular channels in sub-epidermal location, while the solid component present in the deeper dermis. **G–I** (Case 3, dura) EH with focal vasoformative growth composed of sinusoidal, inter-anastomosing pattern (**G**), and large areas of solid growth (**H, I**). Tumor cells show abundant eosinophilic cytoplasm and enlarged nuclei with irregular nuclear contours, open chromatin, small but distinct nucleoli, and mild to moderate nuclear pleomorphism.

One case showed a focal spindle cell component, composed of bland ovoid to short fusiform cells with vesicular nuclei and pale eosinophilic cytoplasm (case #1, Fig. 1). Moreover, most cases lacked blister cells, or intracytoplasmic vacuoles as well as eosinophils. Only one case showed abundant inflammation, which was comprised by sheets of plasma cells and lymphocytes (index case #1; Fig. 1). Only one case showed very rare eosinophils, while none were detected in the remaining four cases. None of the cases showed prominent or distinctive stromal component, such as hyalinization or chondromyxoid extracellular matrix, as seen with other epithelioid vascular lesions.

All except one case showed some degree of cytologic atypia, including nuclear enlargement, mild to moderate cytologic atypia, and prominent nucleoli (Figs. 1 and 2, and Table 1). However, despite these worrisome features, none showed a brisk mitotic activity or necrosis. Overall the lesions had a low mitotic count with 1–2 MF/10 HPFs.

Targeted RNA sequencing using the Archer® FusionPlex® Sarcoma Panel was performed in the index case. The supporting reads covering the fusion junction showed the presence of a fusion transcript composed of *GATA6* (NM_005257) exon 6 fused to *FOXO1* (NM_002015) exon 2 (Fig. 3). This result was also confirmed by FISH. Moreover, FISH break-apart assay performed in the remaining cases showed the presence of *FOXO1* gene rearrangement, as well as come-together signal with *GATA6*, using the FISH fusion assay (Supplementary Fig. 1).

Immunohistochemistry for *FOS* and *FOSB* is negative in the *GATA6-FOXO1* subset of EH

In order to evaluate the potential relationship between our cohort and the more common EH groups with *FOS* or *FOSB* gene rearrangements, we have performed immunohistochemistry for these two markers, using 4- μ m-thick formalin-fixed paraffin-embedded whole-tissue sections,

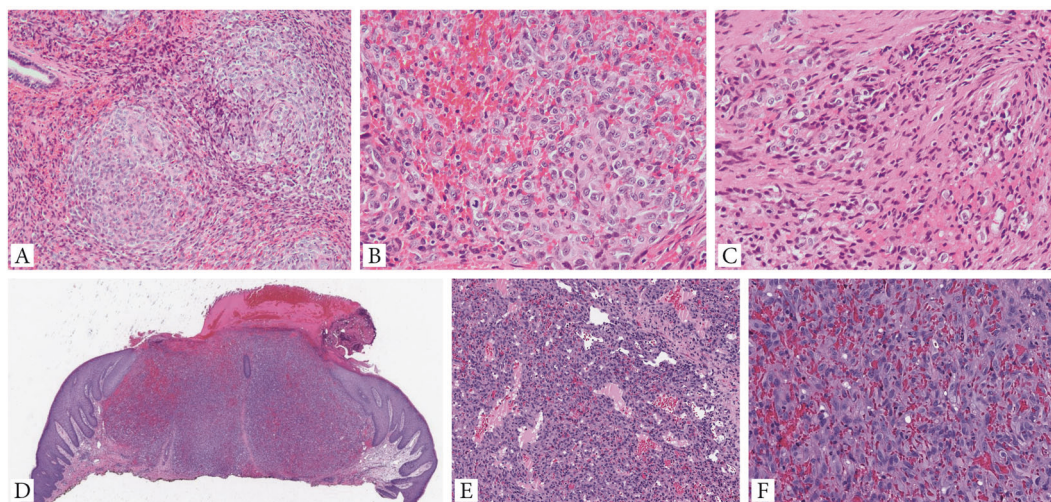


Fig. 2 Additional histologic features of EH with *GATA6-FOXO1* fusions. **A–C** (Case 4) EH involving nasopharyngeal mucosa shows a distinctive multinodular growth (**A**). Higher power shows solid sheets of epithelioid cells with light eosinophilic cytoplasm and enlarged nuclei with mild atypia, vesicular chromatin, and prominent nucleoli. Scattered mitotic figures can be seen, but no necrosis present (**B**). Extravasated red blood cells are seen intermixed within the solid component. A focal spindle cell component is noted (**C**). **D–F**

Cutaneous EH (case 5, back) showing a solid nodular growth, associated with overlying ulceration, and delineated by a vague collarette. Tumor displays a biphasic growth, with alternating vasoformative areas composed of sinusoidal and irregular-contour vascular channels (**E**), and solid components (**F**). The latter finding reveals sheets of plump ovoid to epithelioid cells with abundant eosinophilic cytoplasm and irregular nuclei, with open chromatin and moderate cytologic atypia. No necrosis is identified.

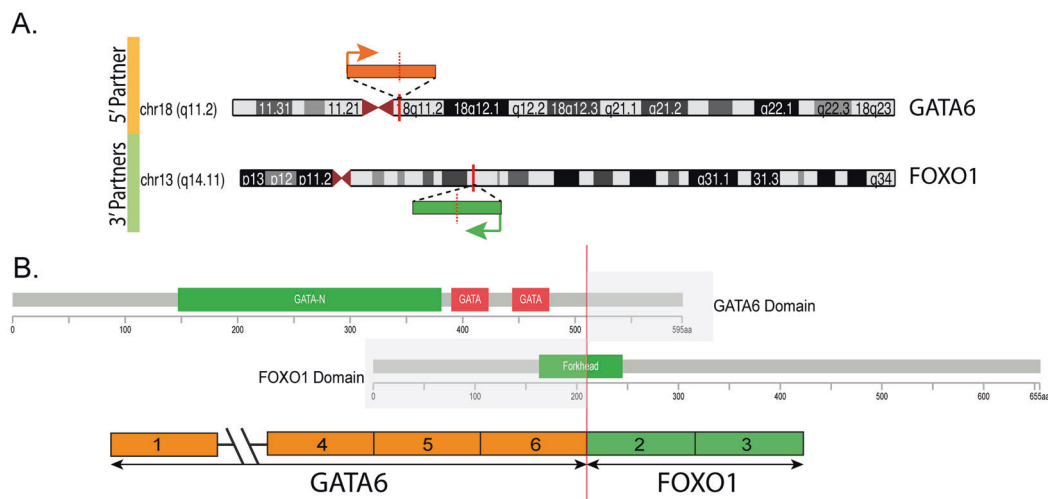


Fig. 3 Molecular characterization of novel *GATA6-FOXO1* fusion. **A** Diagrammatic representation of the chromosomal locations of *GATA6* on 18q11.2 and *FOXO1* on 13q14.11. Vertical red bars indicate the exact genomic break, while orange and green arrows indicate

the direction of transcription for each gene. **B** Breakpoints on the two genes (red vertical line) showing the exonic composition of the fusion transcript and the retained coding regions of the encoded fusion protein. Protein domains are also represented.

following pressure cooker heat-induced epitope retrieval. Immunohistochemistry for FOSB was performed using Target Retrieval Solution (pH 6.1; Dako, Carpinteria, CA), and a rabbit monoclonal antibody (1:2000 dilution, clone 5G4; Cell Signaling Technology, Danvers, MA) and the Envision Plus detection system (Dako), as previously reported [17]. For the FOS immunohistochemistry, we used a polyclonal c-FOS antibody targeting the N-terminus (1:500 dilution; clone ABE457, Merck Millipore, MA) [18].

Clinical and histologic features of fusion-negative EHs

Twenty-three EH cases were negative for *GATA6* and *FOXO1* gene rearrangements by FISH. This molecular negative cohort included the following locations: eight soft tissue extremities, two skin, six head and neck, five bone, and two visceral (testis). No distinct differences in morphology were noted with the fusion-positive group,

although most cases showed more overt vasof ormation and readily identifiable intracytoplasmic vacuoles. In addition, all six ALHE cases tested were negative for *GATA6* and *FOXO1* gene abnormalities.

Discussion

In this study, we report a small series of five EH lesions associated with a novel *GATA6-FOXO1* fusions. The tumors occurred in young adults with no gender predilection, with three cases occurring in the head and neck location. Tumors showed mostly a superficial location, involving either skin or subcutis, and had an intravascular growth in one case arising in the leg. Their clinical presentation is somewhat distinct from the more common molecular subsets of EH associated with either *FOS* or *FOSB* gene fusions, which occur preferentially in the bone, deep-seated soft tissues, and outside the head and neck location [11–13].

The morphologic spectrum of EH exhibits a wide range of appearances, including cellular/solid proliferation, atypical cytomorphology, prominent inflammatory infiltrate, and intravascular growth [19]. Due to this diverse histomorphologies, the diagnosis of EH remains challenging, being confused at one end of the spectrum with inflammatory conditions (e.g., Kimura disease), while at the other end with malignant epithelioid vascular tumors, such as EHE and epithelioid AS [20]. Moreover, the distinction from malignant lesions is further complicated by the aggressive clinical presentation, mostly encountered with intraosseous EH, showing destructive growth and/or multifocality [8]. The current study group showed significant histologic overlap with the *FOS* and *FOSB* rearranged EH, including alternating solid and vasoformative component, predominant epithelioid cytomorphology, hemorrhagic changes within the stroma. However, the *GATA6-FOXO1*-molecular subset of EH rarely exhibited blister cells or evidence of intracytoplasmic vacuoles, tombstone pattern, or a stromal eosinophilic infiltrate. Atypical histologic features have been previously described in the setting of EH, especially those associated with *ZFP36-FOSB* fusions, which often showed solid components with increased cellularity, the presence of mild to moderate degree of nuclear pleomorphism and areas of necrosis [12]. Similarly, some of the cases in our study group showed areas of solid growth and cytologic atypia, but lacked increased mitotic activity or necrosis.

It is intriguing to speculate that some gene fusions are more prone to occur in certain anatomic locations, with *FOS*-related fusions being common in EH of bone [11, 13], *FOSB* in the penis [12], and *GATA6-FOXO1* fusions showing a preferential distribution in the skin, and head and

neck. Of note, the initial descriptions of EH, albeit described under different terminologies, including ALHE, showed a predilection for the skin, and subcutis of the head and neck [3–5, 7]. Recent molecular studies have shown that lesions in the morphologic spectrum of ALHE, typically defined by variable epithelioid endothelial cells associated with a vascular “blow-out” pattern and prominent inflammation, including eosinophils, do not harbor *FOS* and *FOSB* fusions [11]. Our current study, however, highlights the heterogeneity of the vascular lesions with epithelioid endothelial changes occurring in the skin, and head and neck, by identifying a small subset with novel fusions, which highly resembles classic EH rather than ALHE. Moreover, the current subset did not show an enriched inflammatory component in eosinophils, as commonly seen in ALHE.

GATA6 is the only member of the GATA family of zinc-finger transcription factors expressed in vascular smooth muscle cell, being involved in inhibiting proliferation and promoting a contractile phenotype [21]. Some of the *GATA6* target genes include genes encoding the angiotensin type 1 receptor, endothelin-1, and vascular cell adhesion molecule-1. The role of *GATA6* in cancer remains under investigation, being different in different organs and tissues, with both tumor suppressor and oncogenic roles being proposed [22].

As *FOS* and *FOSB*-related fusions are the common genetic alterations seen in EH, we further investigated our cohort using immunohistochemistry for these antibodies for a potential shared pathogenic relationship. However, none of the cases showed positivity. Moreover, *FOSB* fusions have been also described in a different vascular neoplasm, pseudomyogenic hemangioendothelioma (PHE), which can display a mixture of spindle and epithelioid phenotype, and may be considered in the differential diagnosis [23]. However, PHE typically lack any evidence of vasof ormation and are associated with a fibrotic rather than hemorrhagic and inflammatory background.

In contrast, *FOXO1* transcription factor has been well documented to be involved in a number of fusions driving mesenchymal neoplasms. *FOXO1* fusions with either *PAX3* and *PAX7* represent the molecular hallmark of alveolar rhabdomyosarcomas [1]. Moreover, *FOXO1* fusions associated with *SRF* have been reported in a distinctive subset of well-differentiated rhabdomyosarcoma [24]. And more recently, a single case report of a *OGT-FOXO1* fusion was described in a so-called “myoepithelioma-like hyalinizing epithelioid tumor”, arising in the foot of a 40-year-old female [25]. However, our report appears to be the first example of *FOXO1*-related fusions driving the pathogenesis of an endothelial neoplasm. *FOXO1* belongs to the forkhead box protein O (FoxO) transcription factor family, and typically retains its transactivation domain (TAD) in the

fusion oncoprotein. FOXO1 has important roles in regulating proliferation and differentiation of various cell types [26].

The index case showed the fusion of two transcription factors, GATA6 and FOXO1, similar to the *PAX3-FOXO1* fusion in alveolar rhabdomyosarcoma [27]. In the latter fusion event, the DNA-binding sites of PAX3 are retained and thus enable FOXO1-mediated stimulation of a multitude of known target genes across the genome [28, 29]. Interestingly, in the *GATA6-FOXO1* fusion event, all functional domains of the GATA6 protein are retained, including its DNA-binding sites. FOXO1, however, is truncated: only the distal half of the forkhead DNA-binding domain (DBD), as well as the other C-terminal domains, including nuclear localization, nuclear export signal, and the TAD are retained [30, 31]. The loss of the N-terminal FOXO1 sequence prevents PKB/Akt phosphorylation at the conserved region 1, thereby abrogating negative regulation of transcriptional activity, and may also negatively affect DNA binding. We noted a similar genetic phenomenon in a couple of other *GATA6* fusion events reported in the scientific literature [32–34]. Notably, these occurred in different tumor types and with different fusion partners. Collectively, these observations suggest a chimeric fusion protein that hijacks DBDs of GATA6 and may use catalytic properties of both proteins. Functional studies are required to investigate this further.

In summary, this study identified a novel molecular EH subset, which occurs at various anatomic locations and spans a wide morphologic spectrum, including atypical features that can mimic malignant vascular tumors. Of interest none of these lesions occurred in the bone, a common site for EH, which are often characterized by *FOS* and *FOSB* fusions. Although overall findings are in keeping with an EH family of tumors, this subset displayed somewhat distinct features, including a predominant solid growth, paucity of blister cells, and lacked the characteristic tombstone nuclear projection of endothelial nuclei into the lumen. Despite lack of brisk mitotic activity or necrosis, most lesions showed enlarged nuclei with small, but prominent nucleoli and mild to moderate nuclear pleomorphism, worrisome for a malignant process. This study illustrates the practical utility of RNA sequencing in classifying challenging neoplasms by identifying novel gene fusions. Further studies are clearly necessary to establish the relationship of this molecular subset with the more common EH with *FOS* and *FOSB* gene fusions.

Acknowledgements We are very thankful for Dr. Jason Hornick assistance with the *FOSB* immunohistochemistry, which was performed at Brigham and Women's Hospital, Boston, MA. We are also grateful to Dr. Achim Jungbluth and Denise Frosina for the *FOS* immunohistochemistry. We also thank Bruce Crilly for his assistance with image composites and Milagros Soto for editorial support.

Funding This work was supported in part by P50 CA 140146-01 (to CRA), P50 CA217694 (to CRA), P30 CA008748 (to CRA), Cycle for Survival (to CRA), Kristin Ann Carr Foundation (to CRA), EHE Foundation (to CRA).

Compliance with ethical standards

Conflict of interest The authors declare that they have no conflict of interest.

Publisher's note Springer Nature remains neutral with regard to jurisdictional claims in published maps and institutional affiliations.

References

1. WHO. Who Classification of Tumors. Editorial Board. Soft tissue and bone tumors, Vol. 3, 5th ed. Lyon: IARC; 2020.
2. Rosai J, Akerman LR. Intravenous atypical vascular proliferation. A cutaneous lesion simulating a malignant blood vessel tumor. *Arch Dermatol.* 1974;109:714–7.
3. Castro C, Winkelmann RK. Angiolymphoid hyperplasia with eosinophilia in the skin. *Cancer.* 1974;34:1696–705.
4. Fetsch JF, Sesterhenn IA, Miettinen M, Davis CJ Jr. Epithelioid hemangioma of the penis: a clinicopathologic and immunohistochemical analysis of 19 cases, with special reference to exuberant examples often confused with epithelioid hemangioendothelioma and epithelioid angiosarcoma. *Am J Surg Pathol.* 2004;28:523–33.
5. Fetsch JF, Weiss SW. Observations concerning the pathogenesis of epithelioid hemangioma (angiolymphoid hyperplasia). *Mod Pathol.* 1991;4:449–55.
6. Jones EW, Bleehen SS. Inflammatory angiomatous nodules with abnormal blood vessels occurring about the ears and scalp (pseudotumor or atypical pyogenic granuloma). *Br J Dermatol.* 1969;81:804–16.
7. Rosai J, Gold J, Landy R. The histiocytoid hemangiomas. A unifying concept embracing several previously described entities of skin, soft tissue, large vessels, bone, and heart. *Hum Pathol.* 1979;10:707–30.
8. Errani C, Zhang L, Panicek DM, Healey JH, Antonescu CR. Epithelioid hemangioma of bone and soft tissue: a reappraisal of a controversial entity. *Clin Orthop Relat Res.* 2012;470:1498–506.
9. Evans HL, Raymond AK, Ayala AG. Vascular tumors of bone: a study of 17 cases other than ordinary hemangioma, with an evaluation of the relationship of hemangioendothelioma of bone to epithelioid hemangioma, epithelioid hemangioendothelioma, and high-grade angiosarcoma. *Hum Pathol.* 2003;34:680–9.
10. Nielsen GP, Srivastava A, Kattapuram S, Deshpande V, O'Connell JX, Mangham CD, et al. Epithelioid hemangioma of bone revisited: a study of 50 cases. *Am J Surg Pathol.* 2009;33:270–7.
11. Huang SC, Zhang L, Sung YS, Chen CL, Krausz T, Dickson BC, et al. Frequent *FOS* gene rearrangements in epithelioid hemangioma: a molecular study of 58 cases with morphologic reappraisal. *Am J Surg Pathol.* 2015;39:1313–21.
12. Antonescu CR, Chen HW, Zhang L, Sung YS, Panicek D, Agaram NP, et al. ZFP36-FOSB fusion defines a subset of epithelioid hemangioma with atypical features. *Genes Chromosomes Cancer.* 2014;53:951–9.
13. van IDG, de Jong D, Romagosa C, Picci P, Benassi MS, Gambarotti M, et al. Fusion events lead to truncation of *FOS* in epithelioid hemangioma of bone. *Genes Chromosomes Cancer.* 2015;54:565–74.
14. Pfarr N, Stenzinger A, Penzel R, Warth A, Dienemann H, Schirmacher P, et al. High-throughput diagnostic profiling of clinically actionable gene fusions in lung cancer. *Genes Chromosomes Cancer.* 2016;55:30–44.

15. Endris V, Penzel R, Warth A, Muckenhuber A, Schirmacher P, Stenzinger A, et al. Molecular diagnostic profiling of lung cancer specimens with a semiconductor-based massive parallel sequencing approach: feasibility, costs, and performance compared with conventional sequencing. *J Mol Diagn.* 2013;15:765–75.
16. Kirchner M, Neumann O, Volckmar AL, Stogbauer F, Allgauer M, Kazdal D, et al. RNA-based detection of gene fusions in formalin-fixed and paraffin-embedded solid cancer samples. *Cancers.* 2019;11:1309.
17. Hung YP, Fletcher CD, Hornick JL. FOSB is a useful diagnostic marker for pseudomyogenic hemangioendothelioma. *Am J Surg Pathol.* 2017;41:596–606.
18. Amary F, Markert E, Berisha F, Ye H, Gerrand C, Cool P, et al. FOS expression in osteoid osteoma and osteoblastoma: a valuable ancillary diagnostic tool. *Am J Surg Pathol.* 2019;43:1661–67.
19. Luzar B, Ieremia E, Antonescu CR, Zhang L, Calonje E. Cutaneous intravascular epithelioid hemangioma. A clinicopathological and molecular study of 21 cases. *Mod Pathol.* 2020;33:1527–36.
20. Antonescu C. Malignant vascular tumors-an update. *Mod Pathol.* 2014;27 Suppl 1:S30–8.
21. Lepore JJ, Cappola TP, Mericko PA, Morrissey EE, Parmacek MS. GATA-6 regulates genes promoting synthetic functions in vascular smooth muscle cells. *Arterioscler Thromb Vasc Biol.* 2005;25:309–14.
22. Sun Z, Yan B. Multiple roles and regulatory mechanisms of the transcription factor GATA6 in human cancers. *Clin Genet.* 2020;97:64–72.
23. Agaram NP, Zhang L, Cotzia P, Antonescu CR. Expanding the spectrum of genetic alterations in pseudomyogenic hemangioendothelioma with recurrent novel ACTB-FOSB gene fusions. *Am J Surg Pathol.* 2018;42:1653–61.
24. Karanian M, Pissaloux D, Gomez-Brouchet A, Chevenet C, Le Loarer F, Fernandez C, et al. SRF-FOXO1 and SRF-NCOA1 fusion genes delineate a distinctive subset of well-differentiated rhabdomyosarcoma. *Am J Surg Pathol.* 2020;44:607–16.
25. Yorozu T, Nagahama K, Morii T, Maeda D, Yoshida A, Mori T, et al. Myoepithelioma-like hyalinizing epithelioid tumor of the foot harboring an OGT-FOXO1 fusion. *Am J Surg Pathol.* 2020.
26. Eijkelenboom A, Burgering BM. FOXOs: signalling integrators for homeostasis maintenance. *Nat Rev Mol Cell Biol.* 2013;14:83–97.
27. Fredericks WJ, Galili N, Mukhopadhyay S, Rovera G, Bennicelli J, Barr FG, et al. The PAX3-FKHR fusion protein created by the t(2;13) translocation in alveolar rhabdomyosarcomas is a more potent transcriptional activator than PAX3. *Mol Cell Biol.* 1995;15:1522–35.
28. Wachtel M, Schafer BW. PAX3-FOXO1: zooming in on an “undruggable” target. *Semin Cancer Biol.* 2018;50:115–23.
29. Linardic CM. PAX3-FOXO1 fusion gene in rhabdomyosarcoma. *Cancer Lett.* 2008;270:10–8.
30. Psenakova K, Kohoutova K, Obsilova V, Ausserlechner MJ, Veverka V, Obsil T. Forkhead domains of FOXO transcription factors differ in both overall conformation and dynamics. *Cells.* 2019;8:966.
31. Obsil T, Obsilova V. Structure/function relationships underlying regulation of FOXO transcription factors. *Oncogene.* 2008;27:2263–75.
32. Klijn C, Durinck S, Stawiski EW, Haverty PM, Jiang Z, Liu H, et al. A comprehensive transcriptional portrait of human cancer cell lines. *Nat Biotechnol.* 2015;33:306–12.
33. Gao Q, Liang WW, Foltz SM, Mutharasu G, Jayasinghe RG, Cao S, et al. Driver fusions and their implications in the development and treatment of human cancers. *Cell Rep.* 2018;23:227–38 e3.
34. Hu X, Wang Q, Tang M, Barthel F, Amin S, Yoshihara K, et al. TumorFusions: an integrative resource for cancer-associated transcript fusions. *Nucleic Acids Res.* 2018;46:D1144–D49.